MODELLING AND CONTROL OF A VEHICLE WITH SINGLE-WHEEL CHASSIS ACTUATORS

Ralf Orend

Lehrstuhl für Regelungstechnik
Universität Erlangen-Nürnberg
Cauerstraße 7, 91058 Erlangen, Germany
ralf.orend@rt.eei.uni-erlangen.de

Abstract: For a vehicle equipped with active single-wheel steering, brake, drive and suspension systems a nonlinear vehicle model is presented. On the basis of this model an integrated vehicle dynamics control is developed comprising all of the mentioned chassis actuators to control the plane vehicle motion. The basic control strategy consists in two parts. One part is a flatness based tracking controller for the vehicle motion, delivering a yaw moment and forces in longitudinal and lateral direction as control commands. The other part is an analytical allocation of these control commands into adequate commands for the chassis actuators, i.e. steer angles, wheel speeds and a wheel load intervention.

Keywords: automotive control, vehicle dynamics, chassis control, nonlinear control, model-based control

1. INTRODUCTION

This contribution deals with the longitudinal and lateral dynamics of a vehicle equipped with active single-wheel chassis actuators, i.e. single-wheel steering, brake, drive and suspension systems. Thus the steering angle and the brake resp. drive torque at each single wheel are controlled individually. Moreover the wheel load distribution is influenced by active wheel load interventions. All in all this provides the possibility to control the tyre forces at each single wheel independently up to the limit of adhesion with the view to achieve a desired plane vehicle motion.

With regard to this constellation an appropriate vehicle model is developed. Its main feature is that it can be inverted analytically, i.e. one can calculate the steering angles and the wheel speeds from the desired vehicle motion. On the basis of this model a strategy is derived to control the plane vehicle motion comprising all of the mentioned single-wheel chassis actuators.

The aim of this contribution is to present a structured procedure to design a model-based integrated vehicle dynamics control for a vehicle equipped with active single-wheel steering, brake, drive and suspension systems.

The paper is organized as follows: The nonlinear vehicle model is presented in Sec. 2. In Sec. 3 the control strategy is derived and an appropriate controller design is carried out. In Sec. 4 the efficiency of the designed integrated vehicle dynamics control is finally tested in computer simulations.

2. VEHICLE MODEL

The longitudinal and lateral vehicle dynamics are described by a nonlinear twotrack vehicle model. The vehicle is assumed to behave like a rigid body moving on a plane road. Vertical dynamic

effects, like roll, pitch and heave movements will not be considered; they are supposed to be either compensated by the active suspension system or are suppressed by an appropriate mechanical design of the wheel suspension.

2.1 Dynamics of the plane vehicle motion

The plane vehicle motion is specified by the yaw rate $\dot{\psi}$, the sideslip angle β and the vehicle velocity v. These three variables of motion are determined by the resulting yaw moment M_z, the resulting longitudinal force F_x and the resulting lateral force F_y acting on the vehicle with its mass m and its yaw moment of inertia J_z.

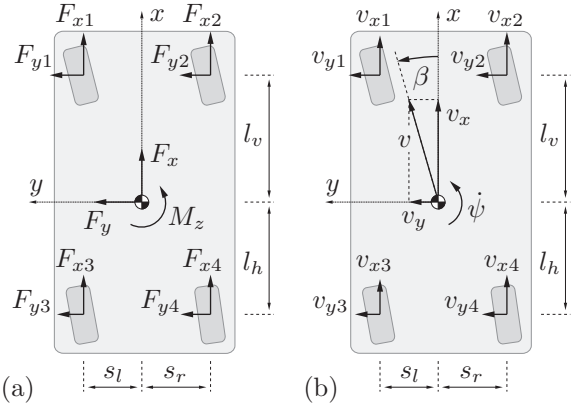

Fig. 1. Schematic depiction of a plane vehicle motion: (a) forces and moments, (b) velocities

Regarding the vehicle-fixed coordinate system (which is rotating with the angular speed $\dot{\psi}$ relativ to a road-fixed inertial system) the basic equations of the plane vehicle motion can be written as follows (cf. Fig. 1):

$$\underbrace{\frac{d}{dt}\begin{bmatrix}\dot{\psi}\\ v_x\\ v_y\end{bmatrix}}_{\dot{x}} = \underbrace{\begin{bmatrix}0\\ v_y\dot{\psi}\\ -v_x\dot{\psi}\end{bmatrix}}_{f(x)} + \underbrace{\begin{bmatrix}\frac{1}{J_z} & 0 & 0\\ 0 & \frac{1}{m} & 0\\ 0 & 0 & \frac{1}{m}\end{bmatrix}}_{B}\underbrace{\begin{bmatrix}M_z\\ F_x\\ F_y\end{bmatrix}}_{u}, \tag{1}$$

$$\underbrace{\begin{bmatrix}\dot{\psi}\\ \beta\\ v\end{bmatrix}}_{y} = \underbrace{\begin{bmatrix}\dot{\psi}\\ \arctan\frac{v_y}{v_x}\\ \sqrt{v_x^2+v_y^2}\end{bmatrix}}_{h(x)}, \quad \underbrace{\begin{bmatrix}\dot{\psi}\\ v_x\\ v_y\end{bmatrix}}_{x} = \underbrace{\begin{bmatrix}\dot{\psi}\\ v\cos\beta\\ v\sin\beta\end{bmatrix}}_{h^{-1}(y)}$$

with the longitudinal and lateral velocity $v_x > 0$ resp. v_y of the center of gravity of the vehicle.

Neglecting external disturbances, e.g. air resistance, the resulting yaw moment and the resulting longitudinal and lateral force $u = \begin{bmatrix}M_z & F_x & F_y\end{bmatrix}^{\mathrm{T}}$ are generated by longitudinal and lateral tyre forces F_{xi} resp. F_{yi} (cf. Fig. 1a):

$$u = \underbrace{\begin{bmatrix}-s_l & l_v & s_r & l_v & -s_l & -l_h & s_r & -l_h\\ 1 & 0 & 1 & 0 & 1 & 0 & 1 & 0\\ 0 & 1 & 0 & 1 & 0 & 1 & 0 & 1\end{bmatrix}}_{G} F_{xy}\,, \tag{2}$$

$$F_{xy}^{\mathrm{T}} = \begin{bmatrix}F_{x1} & F_{y1} & F_{x2} & F_{y2} & F_{x3} & F_{y3} & F_{x4} & F_{y4}\end{bmatrix}.$$

The longitudinal and lateral velocities at the wheel centers v_{xi} resp. v_{yi} are given by (cf. Fig. 1b):

$$v_{xy} = \begin{bmatrix}v_{x1} & v_{y1} & v_{x2} & v_{y2} & v_{x3} & v_{y3} & v_{x4} & v_{y4}\end{bmatrix}^{\mathrm{T}} = \underbrace{\left(\begin{bmatrix}\dot{\psi} & v\cos\beta & v\sin\beta\end{bmatrix} G\right)^{\mathrm{T}}}_{g(y)}. \tag{3}$$

Remark 1: Throughout the text the index i refers to the respective wheel of the vehicle (e.g. v_{xi}):

front left: $i = 1$ front right: $i = 2$
rear left: $i = 3$ rear right: $i = 4$

2.2 Distribution of the wheel loads

Due to the fact that the tyre forces are acting on road level, i.e. with a lever to the center of gravity of the vehicle, roll and pitch moments are generated. As no vertical vehicle motion is assumed to occur, there has to be a static force and moment equilibrium (cf. Fig. 2)

$$\begin{bmatrix}mg\\ hF_x\\ hF_y\end{bmatrix} = \underbrace{\begin{bmatrix}1 & 1 & 1 & 1\\ -l_v & -l_v & l_h & l_h\\ -s_l & s_r & -s_l & s_r\end{bmatrix}}_{V}\underbrace{\begin{bmatrix}F_{z1}\\ F_{z2}\\ F_{z3}\\ F_{z4}\end{bmatrix}}_{F_z} \tag{4}$$

with the wheel loads F_{zi} and the sums of the longitudinal and lateral tyre forces F_x resp. F_y.

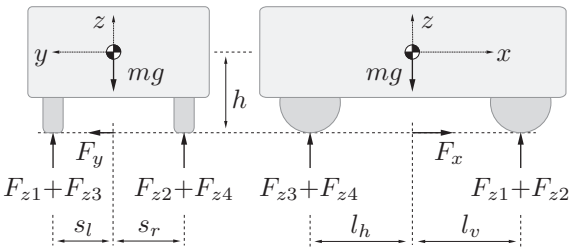

Fig. 2. Vertical force and moment equilibrium

This leads to the wheel load distribution

$$F_z = \underbrace{V^{+}\left(\begin{bmatrix}mg\\ 0\\ 0\end{bmatrix} + h\begin{bmatrix}0 & 0 & 0\\ 0 & 1 & 0\\ 0 & 0 & 1\end{bmatrix}u\right)}_{z(u)} + n_V\,\Delta F_z \tag{5}$$

with the Moore-Penrose inverse (see e.g. (Ben-Israel and Greville, 2003)) and a kernel of V

$$V^+ = V^{\mathrm{T}}(VV^{\mathrm{T}})^{-1},\ n_V = \begin{bmatrix}1 & -1 & -1 & 1\end{bmatrix}^{\mathrm{T}} \quad (6)$$

and an arbitrary parameter ΔF_z.

For a vehicle with passive suspension, the parameter ΔF_z is firmly specified by the mechanical setup of the chassis, i.e. particularly by anti-roll bars. Regarding a vehicle with an active suspension system, one is able to control the wheel load intervention ΔF_z to achieve a desired wheel load distribution subject to the driving situation (see e.g. (Smakman, 2000)).

2.3 The tyre-road contact

The modelling of the tyre-road contact is crucial in every vehicle model, since it is the point where the tyre forces are determined. The paper at hand acts on the maxime to account for the important aspects, but to keep it as simple as possible. The considered features are force saturation, combined slip, degressive dependency on the wheel load and dependency on the friction coefficient.

For the sake of simplicity an isotropic tyre behaviour is assumed (see e.g. (Burckhardt, 1993)), i.e. the tyre force F_i and the tyre slip s_i point in the same direction and the magnitude of the tyre force is independent of its direction (cf. Fig. 4). Therefore the tyre slip is considered as a vector that is caused by a relativ velocity at the contact patch between tyre belt and road. It is quantified by the following definition which is a vectorial interpretation of the usual scalar definition:

$$\begin{aligned} s_i &= -\frac{1}{\|v_i\|}\Delta v_i = \underbrace{-\frac{1}{\|v_i\|}}_{r_{si}(\delta_i,\omega_i;v_i)}(v_{ci}+v_i)\ , \\ v_{ci} &= -r_i\omega_i\begin{bmatrix}\cos\delta_i & \sin\delta_i\end{bmatrix}^{\mathrm{T}} \end{aligned} \quad (7)$$

with the velocity v_{ci} at the circumference of the wheel, the velocity $v_i = \begin{bmatrix}v_{xi} & v_{yi}\end{bmatrix}^{\mathrm{T}}$ at the wheel center, the steering angle δ_i, the wheel speed $\omega_i \geq 0$ and the effective free rolling radius r_i (cf. Fig. 3).

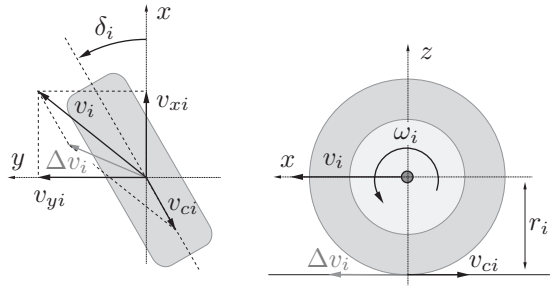

Fig. 3. Wheel velocity and speed

The following approach for the relation between tyre force, tyre slip and wheel load is motivated by the basic equations of the well known "Magic tyre formula" (see e.g. (Pacejka and Besselink, 1997)). The influence of the friction coefficient is thereby included as proposed in e.g. (Ammon, 1997).

The tyre force $F_i = \begin{bmatrix}F_{xi} & F_{yi}\end{bmatrix}^{\mathrm{T}}$ and the adhesion limit, i.e. the peak value of the tyre force are specified by:

$$F_i = \underbrace{\bar{F}_i \sin\left(C_i \arctan\left(B_i\frac{\|s_i\|}{\mu_i}\right)\right)\frac{1}{\|s_i\|}}_{r_{Fi}(s_i;F_{zi})} s_i\ , \quad (8)$$

$$\bar{F}_i = \mu_i F_{zi}\left(1 + k_{Fz,i}\frac{F_{z0,i}-F_{zi}}{F_{z0,i}}\right) (\geq 0) \quad (9)$$

with the friction coefficient between tyre and road μ_i and the tyre parameters $B_i > 0$, $C_i > 1$, $k_{Fz,i} \geq 0$, $F_{z0,i} > 0$.

The resulting tyre characteristics are schematically depicted in Fig. 4.

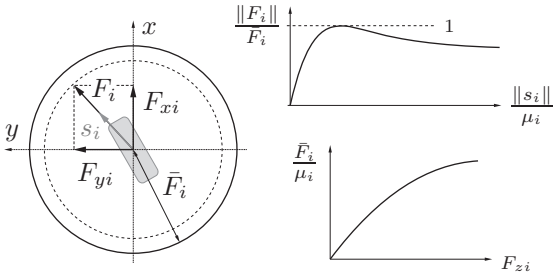

Fig. 4. Isotropic tyre behaviour with its basic characteristics

2.4 Complete nonlinear vehicle model

For a better overview of the complete vehicle model, the prior results are compactly depicted in Fig. 5. Therefore the wheel individual nonlinear scalar functions in (7) resp. (8) and the according scalar variables are merged in vectors:

$$\begin{aligned} r_s &= \begin{bmatrix}r_{s1} & r_{s2} & r_{s3} & r_{s4}\end{bmatrix}^{\mathrm{T}} \\ r_F &= \begin{bmatrix}r_{F1} & r_{F2} & r_{F3} & r_{F4}\end{bmatrix}^{\mathrm{T}} \end{aligned} \quad \left| \begin{aligned} \delta &= \begin{bmatrix}\delta_1 & \delta_2 & \delta_3 & \delta_4\end{bmatrix}^{\mathrm{T}} \\ \omega &= \begin{bmatrix}\omega_1 & \omega_2 & \omega_3 & \omega_4\end{bmatrix}^{\mathrm{T}} \\ s_{xy} &= \begin{bmatrix}s_1 & s_2 & s_3 & s_4\end{bmatrix}^{\mathrm{T}} \end{aligned} \right.$$

3. CONTROL STRATEGY

On the basis of the developed system description of the vehicle, an appropriate control strategy is derived. Therefor it is useful to take a closer look at the basic nature of the vehicle model. It consists in the dynamic subsystem S_{dyn} that is fed back and actuated by the static subsystem S_{stat} (cf. Fig. 5). Starting from this insight the following control strategy is proposed (cf. Fig. 6).

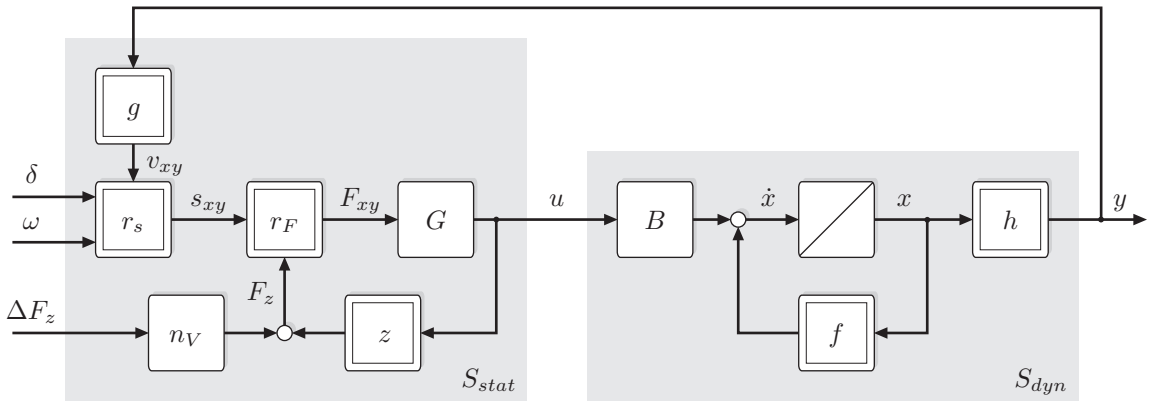

Fig. 5. Block diagram of the complete nonlinear vehicle model

The static subsystem S_{stat} is compensated by its inverse S_{stat}^{-1} for the purpose of achieving a desired yaw moment and a desired longitudinal and lateral force, i.e. $u = u_d$. The remaining dynamic subsystem S_{stat} is controlled by a feedback tracking controller C_T in order to track a desired vehicle motion y_d.

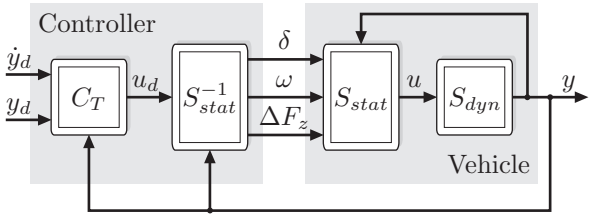

Fig. 6. Schematic depiction of the control strategy

The basic idea behind this strategy is to design a motion controller C_T that uses yaw moment and longitudinal and lateral force as control variables which are translated by S_{stat}^{-1} into control commands for the chassis actuators. In doing so, the desired moment and forces u_d are allocated to steering angles δ, wheel speeds ω and a wheel load intervention ΔF_z.

Remark 2: This paper acts on the assumption that the wheel speeds are controlled by underlying wheel speed controllers that operate active brake and drive systems.

3.1 Inversion of the static subsystem

The inversion of the static nonlinearity S_{stat} is accomplished gradually by the following steps. The steering angle δ_i and the wheel speed ω_i at each single wheel are derived from (7):

$$\delta_i = \arctan\left(\frac{\begin{bmatrix}0 & 1\end{bmatrix}(s_i\|v_i\| + v_i)}{\begin{bmatrix}1 & 0\end{bmatrix}(s_i\|v_i\| + v_i)}\right), \qquad (10)$$

$$\omega_i = \frac{1}{r_i}\|s_i\|v_i\| + v_i\|. \qquad (11)$$

The wheel center velocity $v_i = \begin{bmatrix}v_{xi} & v_{yi}\end{bmatrix}^{\mathrm{T}}$ follows from the measured vehicle motion y according to (3), and the tyre slip s_i is derived from (8):

$$s_i = \frac{\mu_i}{B_i}\tan\left(\frac{1}{C_i}\arcsin\frac{\|F_i\|}{\bar{F}_i}\right)\frac{1}{\|F_i\|}F_i. \qquad (12)$$

The adhesion limit $\bar{F}_i$ is determined by the wheel load F_{zi} (see (9)) which results from (5) subject to the desired moment and forces $u = u_d$:

$$\begin{bmatrix}F_{z1} & F_{z2} & F_{z3} & F_{z4}\end{bmatrix}^{\mathrm{T}} = F_z = z(u) + n_V\,\Delta F_z. \qquad (13)$$

The tyre force $F_i = \begin{bmatrix}F_{xi} & F_{yi}\end{bmatrix}^{\mathrm{T}}$ depends on the desired moment and forces $u = u_d$ and is obtained from the the general solution of (2):

$$\begin{bmatrix}F_1^{\mathrm{T}} & F_2^{\mathrm{T}} & F_3^{\mathrm{T}} & F_4^{\mathrm{T}}\end{bmatrix} = F_{xy} = G^{+}u + N_G\,\Delta F_{xy} \qquad (14)$$

with the Moore-Penrose inverse and a kernel of G

$$G^{+} = G^{\mathrm{T}}(GG^{\mathrm{T}})^{-1},$$
$$N_G = \begin{bmatrix} 1 & 0 & 0 & 0 & -1 & 0 & 0 & 0 \\ 0 & 0 & 1 & 0 & 0 & 0 & -1 & 0 \\ 0 & 1 & 0 & -1 & 0 & 0 & 0 & 0 \\ 0 & 0 & 0 & 0 & 0 & 1 & 0 & -1 \\ -\frac{l}{s} & 0 & \frac{l}{s} & -1 & 0 & 1 & 0 & 0 \end{bmatrix}^{\mathrm{T}}, \qquad (15)$$
$$(l = l_v + l_h\,,\, s = s_l + s_r)$$

and arbitrary parameters ΔF_{xy}. These parameters can be interpreted as tyre forces that have no influence on the resulting yaw moment and the resulting longitudinal and lateral force u, but do affect the distribution of the longitudinal and lateral tyre forces F_{xy}. This is analogous to the wheel load intervention ΔF_z regarding the wheel load distribution F_z (see (13)).

Remark 3: The ratio between the magnitude of the tyre force and its adhesion limit in (12)

$$\eta_i := \frac{\|F_i\|}{\bar{F}_i} \tag{16}$$

represents the utilisation of the adhesion potential of the tyre. By definition the limitations $0 \leq \eta_i \leq 1$ hold for each wheel. For this reason a perfect compensation of S_{stat} is not possible, as these limitations remain and have in fact to be taken into account particularly with regard to the feedback controller design. Nevertheless this difficulty is factored out in this paper.

To determine the yet arbitrary parameters ΔF_{xy} and ΔF_z this study embarks on the strategy to achieve the smallest possible utilisations of the adhesion potentials η_i at all four wheels, thus keeping all tyres as much as possible below their adhesion limit and ensuring an optimal safety reserve in every driving situation. Hence the parameters ΔF_{xy} and the wheel load intervention ΔF_z are determined by an optimisation approach according to (Orend, 2005).

3.2 Tracking control of the dynamic subsystem

After compensating the static subsystem S_{stat} by its inverse S_{stat}^{-1} (cf. Fig. 6) the remaining dynamic subsystem S_{dyn} is considered. It is described by (cf. Fig. 5 and (1))

$$\dot{x} = f(x) + Bu,\ y = h(x). \tag{17}$$

In the following a flatness based analysis of the system (17) is performed. To this end the definition of flatness is recalled (see e.g. (Fliess *et al.*, 1995)). A system is flat, iff there exists a flat output y_f with the following properties:

- I The flat output y_f is a function of the states x, the inputs u and a finit numnber of its time derivatives $\dot{u}, \ddot{u}, ..., u^{(\alpha)}$.
- II The dimension of the flat output y_f equals the dimension of the differential independent components of the inputs u.
- III All system variables, i.e. the states x and the inputs u can be expressed by the flat output y_f and a finit number of its time derivatives $\dot{y}_f, \ddot{y}_f, ..., y_f^{(\gamma)}$.

In the sequel it is shown that the system (17) is flat, i.e. that a flat output is given by:

$$y_f = \begin{bmatrix} y_{f1} \\ y_{f2} \\ y_{f3} \end{bmatrix} = \begin{bmatrix} \dot{\psi} \\ \beta \\ v \end{bmatrix} = y = h(x). \tag{18}$$

Since y_f is a function of x alone condition I is satisfied. Also condition II is met as all components of u are differentially independent, i.e.

$$\operatorname{rank}\left(\frac{\partial(f(x)+Bu)}{\partial u}\right) = \operatorname{rank}(B) = 3 \tag{19}$$

because of $\det(B) = (J_z m^2)^{-1} \neq 0$ (see (1)), and the flat output y_f has the same dimension as u:

$$\dim(y_f) = \dim(y) = \dim(u) = 3. \tag{20}$$

It can be shown that condition III is satisfied as well. The parameterisation of the states x in y_f follows from (1):

$$x = h^{-1}(y_f) = \begin{bmatrix} y_{f1} \\ y_{f3}\cos y_{f2} \\ y_{f3}\sin y_{f2} \end{bmatrix} =: H_x(y_f). \tag{21}$$

Inserting this result in (17), the inputs u can be expressed by y_f as (see (1)):

$$\begin{aligned} u =& B^{-1}(\dot{x} - f(x)) \\ =& B^{-1}\left(\frac{\partial H_x(y_f)}{\partial y_f}\dot{y}_f - f(H_x(y_f))\right) \\ =& \begin{bmatrix} J_z\dot{y}_{f1} \\ m(\dot{y}_{f3}\cos y_{f2} - y_{f3}(y_{f1}+\dot{y}_{f2})\sin y_{f2}) \\ m(\dot{y}_{f3}\sin y_{f2} + y_{f3}(y_{f1}+\dot{y}_{f2})\cos y_{f2}) \end{bmatrix} \\ =& : H_u(y_f, \dot{y}_f). \end{aligned} \tag{22}$$

Given a desired trajectory for the flat output

$$y_{f,d} = y_d = \begin{bmatrix} \dot{\psi}_d & \beta_d & v_d \end{bmatrix}^{\mathrm{T}} \tag{23}$$

the flatness based tracking controller reads

$$u = u_d = H_u(y_f, w),\ w = \dot{y}_{f,d} - Re \tag{24}$$

where

$$R = \operatorname{diag}(R_1, R_2, R_3),\ e = y_f - y_{f,d}. \tag{25}$$

This controller achieves the linear tracking error dynamics $\dot{e} + Re = 0$ for the closed loop system.

Note that the control law (24) consists in a feedforward part $\dot{y}_{f,d}$ and a proportional feedback part Re. The feedback part is done without integral action in order to leave it to the driver to compensate for steady state tracking errors.

4. SIMULATION RESULTS

The efficiency of the designed integrated vehicle dynamics control is tested in computer simulations. As virtual experimental vehicle a more complex and detailled vehicle model of a medium-class car is used showing the following features:

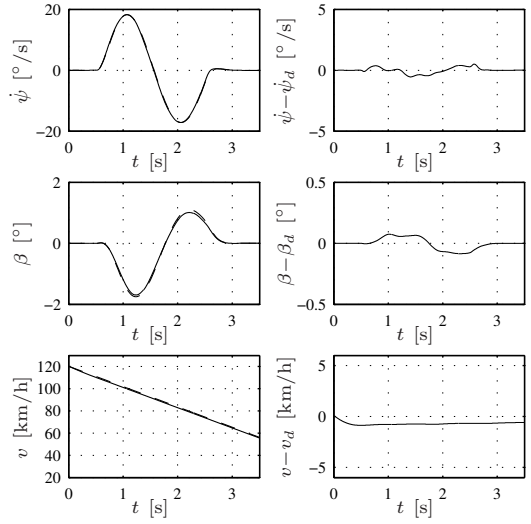

Fig. 7. Simulation results: variables of motion (actual - ; desired - -) and tracking error

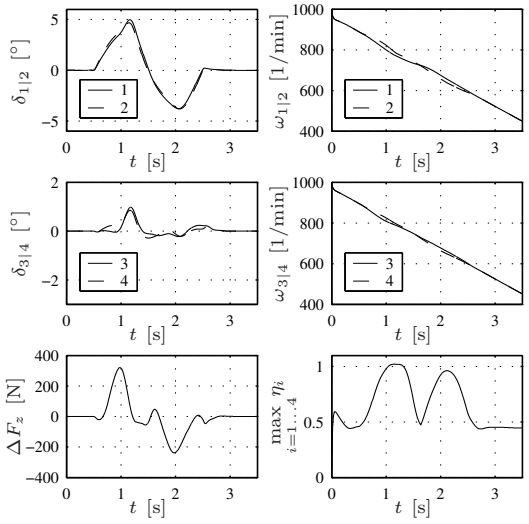

Fig. 8. Simulation results: actuator commands and utilisation of the adhesion potentials

car body motion with all translational and rotational degrees of freedom, suspension kinematics and elastokinematics, wheel rolling and travel motions, tyre dynamics, air resistance, etc. The modelling of the chassis actuators is ideal, i.e. without dynamics and limitations. The wheel speeds are controlled by underlying wheel speed controllers that are yet not further discussed.

Remark 4: In these simulations the active suspension system only takes care of the desired wheel load intervention but does not compensate for vertical movements of the car body, contrary to the assumption made in Sec. 2.

As driving manoeuvre a fast lane change with medium deceleration is examined. The maximum absolut lateral acceleration is 8 m/s^2, and the longitudinal acceleration is kept at a constant value of -5 m/s^2. The desired yaw rate $\dot{\psi}_d$ and the desired sideslip angle β_d are provided by a single-track reference model using a single-sine steer input with a frequency of 0.5 Hz. The desired vehicle velocity v_d starts at 120 km/h and decreases with a constant rate.

The simulation results are depicted in Fig. 7 and Fig. 8. It can be stated that the applied vehicle dynamics control works well since good tracking is achieved. The simulation results show relative small tracking errors with regard to the driving situation: the vehicle is controlled up to its cornering limit, as values of $\eta_i = 1$ are reached.

5. CONCLUSIONS

This contribution showed a structured and analytical approach to handle a multitude of different chassis actuators in order to control the horizontal vehicle motion.

A nonlinear model-based control strategy for a vehicle with single-wheel steering, brake, drive and suspension systems was designed. Therefore in the modelling certain simplifications and assumptions were made concerning mainly the tyre behaviour. By this means one obtained a pragmatic vehicle model that is not too complex and can be inverted analytically, but nevertheless exhibits the essential nonlinear effects of the horizontal vehicle dynamics. It turned out to be a proper basis for a flatness based tracking controller desing that was carried out in the sequel.

The vehicle dynamics control demonstrated its efficiency and performance in computer simulations.

REFERENCES

Ammon, D. (1997). *Modellbildung und Systementwicklung in der Fahrzeugdynamik*. B.G. Teubner. Stuttgart.

Ben-Israel, A. and T.N.E. Greville (2003). *Generalized Inverses*. Springer-Verlag. New York.

Burckhardt, M. (1993). *Fahrwerktechnik: Radschlupfregelsysteme*. Vogel-Verlag. Würzburg.

Fliess, M., J. Levine, P. Martin and P. Rouchon (1995). Flatness and defect of nonlinear systems: Introductory theory and examples. *Int. J. Control 61* pp. 1327 – 1361.

Orend, R. (2005). Vehicle Dynamics Feedforward Control with Optimal Utilisation of the Adhesion Potentials of all four Tyres (in German). *at - Automatisierungstechnik 53* pp. 20 – 27.

Pacejka, H.B. and I.J.M. Besselink (1997). Magic formula tyre model with transient properties. *Vehicle System Dynamics Supplement 27* pp. 234 – 249.

Smakman, H. (2000). *Functional Integration of Slip Control with Active Suspension for Improved Lateral Vehicle Dynamics*. Herbert Utz Verlag. München.